Published in final edited form as:
Biochim Biophys Acta. 2009 January ; 1788(1): 53–63. doi:10.1016/j.bbamem.2008.09.010.

An Introduction to Critical Points for Biophysicists; Observations of Compositional Heterogeneity in Lipid Membranes

Aurelia R. Honerkamp-Smith[1], **Sarah L. Veatch**[2], and **Sarah L. Keller**[1]

[1] Dept. of Chemistry, University of Washington, Seattle WA, 98195-1700, USA

[2] Dept. of Chemistry and Chemical Biology, Cornell University, Ithaca NY, 14853, USA

Abstract

Scaling laws associated with critical points have the power to greatly simplify our description of complex biophysical systems. For the general reader, we first review basic concepts and equations associated with critical phenomena for the general reader. We then apply these concepts to the specific biophysical system of lipid membranes. We recently reported that lipid membranes can contain composition fluctuations that behave in a manner consistent with the two-dimensional Ising universality class. Near the membrane's critical point, these fluctuations are micron-sized, clearly observable by fluorescence microscopy. At higher temperatures, above the critical point, we expect to find submicron fluctuations. In separate work, we have reported that plasma membranes isolated directly from cells exhibit the same Ising behavior as model membranes do. We review other models describing submicron lateral inhomogeneity in membranes, including microemulsions, nanodomains, and mean field critical fluctuations, and we describe experimental tests that may distinguish these models.

Keywords

raft; fluctuation; critical point; two-dimensional Ising; microemulsion; membrane; lipid; cholesterol

---

Biological systems are celebrated for their complexity. One method of rendering biological questions more tractable is to consider broad scaling laws. For example, most animals, independent of their genus, habitat, or ear length, can jump about the same height. Most animals have metabolic rates that scale as rate ~ mass$^{3/4}$. Their leg widths and lengths are related by width ~ length$^{3/2}$. The maximum speed that they can run up a hill scales as mass$^{-1/3}$ ((1) and references within).

The power of simplifying complex systems by applying scaling laws applies beautifully near critical points. Critical phenomena have been applied to a variety of important biological topics, including ion channels (2), neurons (3), protein folding (4; 5), protein phase behavior (6), lipid monolayers (7; 8), lipid bilayers (9–12), evolution (13; 14), social networks (15), and hierarchical organization (16). Many scientists have not encountered the concept of

critical points since their introductory chemistry classes, when they learned that a critical point marks a specific place on the phase diagram of water. Here we compile a brief, self-contained review on critical phenomena in lipid membranes that we wish had existed when we first entered the field. Many expert reviews (17–23) and classic texts (24–26) on critical phenomena and the Ising model exist for scientists with strong backgrounds in physics or physical chemistry. Those readers may wish to skip the basic information contained in the first section of our paper. We intend that this first section will serve as a starting point accessible to the wider biophysical community.

In the remainder of this article, we will review how equations pertaining to critical points predict universal behavior and scaling laws that can be measured in a real biophysical system, a lipid membrane. To do this, we will describe our previously published work showing that equations relevant to a particular simple model, the 2-D Ising model, apply to measurements of nonuniform distributions of lipids in membranes (11; 12). We will also review other descriptions of submicron lateral inhomogeneity in membranes, including microemulsions, nanodomains, and mean field critical fluctuations. We will pay particular attention to how these different models might be distinguished experimentally. Finally, we will review our observations of critical phenomena in lipid membranes isolated from plasma membranes of living cells (11), and speculate on biological implications of these results.

DEFINITIONS AND EQUATIONS

1. Critical points and phase diagrams

The term “critical point” has a meaning more specific than “an important point.” Understanding critical phenomena requires mastering a small set of definitions and equations. Figure 1 shows a phase diagram of water. The critical point lies at the end of the coexistence line between the liquid and vapor. By following line 1, increasing pressure changes the vapor into a liquid. The order parameter is the variable that distinguishes the two phases. Here, the order parameter is density, which is low for the vapor and high for the liquid. In line 2, the phase transition occurs at a critical point. There is no difference between the order parameters of the two phases at the critical point; the densities of the vapor and liquid phases are the same. By following a path around the critical point as in line 3, the fluid continuously changes into a vapor.

Since density is the order parameter, we expect something interesting to happen in a phase diagram drawn so that one axis is a variable related to density, such as molar volume, $\bar{V}$. For example, figure 1b shows a three-dimensional (3-D) phase diagram for water as commonly encountered in freshman chemistry courses. In figure 1b, line 1 does indeed do something interesting at the phase transition. The flat, dashed segment parallel to the $\bar{V}$-axis is a coexistence line, also called a tie-line. This line joins the two phases of different density, vapor and liquid, at constant temperature. As temperature approaches the critical point, this line shrinks until the two endpoints of the line finally merge into a single point at the critical temperature, T_c. Near T_c there is negligible difference in density between the vapor and liquid phases. Within this critical region, the interface energy between the two phases becomes as low as the thermal energy k_BT, which is Boltzmann’s constant times the temperature. As a result, large, thermally-driven fluctuations occur. The fluctuations can be so large that we can see their effects by eye.

2. Observations of Critical Fluctuations

Figure 2 shows a sealed glass tube containing CO_2 near its critical pressure. At room temperature, a meniscus is visible between the vapor and liquid phases. If temperature were increased along a path analogous to line 1 in figure 1, liquid CO_2 would simply boil within the closed tube until only vapor remained. At the critical temperature, instead of boiling, the

meniscus is replaced by a cloudy region that scatters light. This phenomenon, termed critical opalescence, occurs because the sample contains density fluctuations (essentially droplets of liquid in vapor and vice versa) that are the size of the wavelength of light.

As in the 3-D bulk systems described above, critical behavior is also readily observed in two-dimensional (2-D) systems. A 2-D ferromagnet contains an assembly of spins, each of which can be in one of two states (up or down), in analogy to the two states of water described above, liquid or vapor. The salient behavior of 2-D systems very close to critical points is captured by the 2-D Ising model, in which spins on a 2-D lattice communicate only through nearest neighbor interactions. The 2-D Ising model produces a uniform, disordered phase at high temperature, two coexisting phases at low temperature, and fluctuations near the critical point. In later sections, we will see that this same behavior occurs in lipid membranes.

3. Correlation functions and structure factors

Systems near critical points are characterized by the correlation function $G(\vec{r})$, also called the autocorrelation. When the relevant order parameter is density, as for the liquid-vapor transition in CO_2 or water, then one way of representing the (un-normalized) correlation function is:

$$G(\vec{r})=\langle\rho(\vec{r}_0)\rho(\vec{r}_0+\vec{r})\rangle-\langle\rho(\vec{r}_0)\rangle^2. \quad [1]$$

Here, $\rho(\vec{r})$ is the density at position $\vec{r}$ in the sample, and brackets denote an ensemble average. Fluctuations in density are deviations from the average density. The correlation function reflects the probability, given a density fluctuation at position $\vec{r}_0$, of finding a similar fluctuation at a distance $\vec{r}$ away. A random distribution will have a value of $G(\vec{r})=0$ for all $\vec{r}\neq 0$. In the Ising model, local density is replaced by spin state so that the spin-spin correlation is measured. At equilibrium, $G(\vec{r})$ is independent of time, meaning that although individual snapshots of the system may differ, the ensemble average and the distribution of correlations does not change with time. Another commonly measured quantity is the structure factor or power spectrum, $S(\vec{k})$, where $\vec{k}$ is the wavevector in units of inverse length. $S(\vec{k})$ is directly measured in scattering experiments and is the 2-D Fourier transform (*FT*) of $G(\vec{r})$ as follows:

$$S(\vec{k})=\frac{1}{(2\pi)^2}\int d\vec{r}\, G(\vec{r})e^{i\vec{k}\cdot\vec{r}}=FT(G(\vec{r})). \quad [2]$$

In the particular systems we study, correlation function and structure factor are rotationally invariant (12), so angular averages of $G(\vec{r})$ and $S(\vec{k})$ yield $G(r)$ and $S(k)$, respectively.

Correlation functions and structure factors are powerful tools for understanding complex systems because they provide a means to directly compare experiment and theory. $G(r)$ can be calculated directly from statistical mechanics if the interaction energies between molecules are known. Since different forms of interaction energies give rise to different $G(r)$, we can distinguish between possible theories by measuring $G(r)$ or $S(k)$. We will revisit the question of distinguishing alternate theories in later sections. For the moment, we will merely mention that the 2-D Ising model has been solved exactly for the special case of systems near critical points (27).

Correlation functions give rise to correlation lengths, ξ. The value of ξ roughly characterizes the size of the largest structures in a critical system. Figure 3 shows correlation functions for a 2-D Ising model simulation conducted at two temperatures above the critical temperature. Both curves decrease monotonically as r increases, indicating that the system contains many small fluctuations and few large ones. Correlation lengths become larger as the critical point is approached.

The last term that we will define is line tension, λ, which is the 2-D analog of surface tension. Imagine shaking a jar containing oil and water. Droplets of oil form in the water, and vice versa. The droplets are spherical because there is a high surface tension between the oil and water. When two droplets collide, they coalesce into one large droplet.

4. Universality

One of the truly astounding attributes of critical behavior is that it is 'universal,' meaning that many properties can be understood without considering the details of the system. All systems that behave alike belong to the same "universality class". For example, for any system in the Ising universality class, the shape of the curves for $G(r)$ and $S(k)$ depend only on the system's dimensionality and on thermodynamic variables such as temperature and pressure. This means that the same form of correlation functions will be observed for 3-D mixtures of a gas and a liquid (e.g. CO_2), of two partially miscible liquids (e.g. methanol and cyclohexane), or of up and down spins on a lattice (3-D Ising model). The only salient facts are that these systems are near their critical points and that they all belong to the same (3-D Ising) universality class. Similarly, in later sections we will discuss how we have observed the same form of correlation functions for 2-D mixtures of lipids in membranes as have been evaluated for spins on a 2-D lattice (the 2-D Ising model) (11; 12).

One consequence of universality is that correlation lengths, ξ, for every system in the same universality class scale in the same way with temperature, T. As the critical temperature is approached, correlation lengths become large, diverging according to a power law where ν is the critical exponent.

$$\xi=\xi_0\left|\frac{T_c}{T-T_c}\right|^{\nu}=\xi_0\left|\frac{T-T_c}{T_c}\right|^{-\nu} \quad [3]$$

Here, temperature is measured in units of Kelvin. Although the critical exponent ν does not depend on the details of the system, the constant ξ_0 does, and is a length on the order of a single molecule. Other experimental observables such as specific heat or susceptibility follow similar power laws with different critical exponents. For example, the critical exponent μ governs how line tension decreases at the critical point. The critical exponent μ is related to the critical exponent for correlation length, ν, through the number of dimensions in the system, d (25).

$$\lambda=\lambda_0\left|\frac{T-T_c}{T_c}\right|^{\mu} \quad \text{where } \mu=(d-1)\nu \quad [4]$$

For our lipid membrane, $d = 2$. Therefore, $\mu = \nu$. By comparing equations 3 and 4, we expect line tension and correlation length to be inversely related (28).

General power laws and scaling relationships as described above for observables such as correlation length and line tension are a consequence of universality. Specific exponents can

be evaluated by pursuing one of several methods and models such as renormalization group theory, the Ising model, and mean field theory. Renormalization group theory has been reviewed in (26; 29–32). Within the 2-D Ising model, correlation functions for the special case of systems near critical points have been evaluated to produce the exponents in Table 1 (27; 33). The mean field approximation differs from the 2-D Ising model in that it does not take all correlations between fluctuations into account and produces different critical exponents, but is straightforward to solve exactly (23).

As an example of how universality simplifies our description of systems near critical points, consider any two partially miscible liquids such as methanol and cyclohexane. To understand the conditions under which these two liquids mix, simply replace the labels for “vapor” and “liquid” in figure 1c with “liquid 1” and “liquid 2” as in figure 1d, and replace the axis for molar volume with a more appropriate order parameter, the molar fraction of cyclohexane, or “composition”. Liquid 1 is rich in methanol, and liquid 2 is rich in cyclohexane. At low temperature, the liquids do not mix over a range of compositions. The critical point in figure 1d represents the highest temperature at which the two liquids do not completely mix, the “upper consolute point”. Near the critical point, the correlation length of fluctuations in this 3-D system should have a critical exponent of $\nu = 0.63$, just as in the CO_2 system of vapor and liquid.

In our research programs, we investigate miscibility of two liquids in the 2-D system of a lipid bilayer. This bilayer forms a thin shell of a vesicle, enclosing and surrounded by water, as sketched in figure 4a. When the membrane is phase separated below the critical temperature, distinct regions of the membrane are rich in one type of lipid, and the remainder is rich in the other lipids. Again, ‘universality’ lies at the heart of our ability to simplify. It has allowed us to quantitatively analyze composition fluctuations in our complex, multi-component biophysical system using predictions of the simple 2-D Ising model. As described below, we have experimentally demonstrated that correlation lengths in membranes do indeed scale in a manner consistent with the 2-D Ising universality class (11; 12). As physical scientists, we have contributed another entry to the relatively short list of systems within this universality class. As biophysicists, we are excited by the potential connection that our results may establish between statistical mechanics and functional biology.

OBSERVATION OF CRITICAL FLUCTUATIONS IN ‘SIMPLE’ LIPID BILAYERS

We study multi-component membranes in which the lipids separate to form two distinct phases, named “liquid ordered” and “liquid disordered”. Lipid composition distinguishes the two phases, and is the relevant order parameter. Lipid bilayers are thin (~1nm) compared both to the radii of vesicles we study (>10Mm) and to the correlation lengths we resolve by fluorescence microscopy (>0.5μm). Therefore, we expect the behavior of a multi-component lipid bilayer that is very close to its critical point to conform to the 2-D Ising model universality class. Indeed, we recently measured several critical exponents (β, γ, ν, μ) of the lipid bilayers, and found the exponents to be consistent with predictions of the 2-D Ising model (12), and not with predictions of other models, as described in other sections below.

We will review our published results with the aid of figure 5, which shows a small area of a spherical vesicle membrane, imaged over time. The membrane contains a small amount of fluorescent dye, which has a higher concentration in one phase than in the other such that one phase appears dark and the other appears bright. At 19.0°C, a temperature far below the critical temperature of T_c~31.9°C, domain line tension is high. Therefore, domains are circular, and have smooth edges. In figure 5, the domains are bright and the surrounding

membrane is dark. When two domains collide, they coalesce (not shown). As temperature increases toward the critical point, the compositions of the two phases become similar, line tension decreases, and domain edges become rough (10; 12). Above the critical point, no domains persist. Instead, composition fluctuations appear and disappear through time.

We found critical exponents for lipid bilayers to be consistent with exponents predicted by the 2D Ising model as detailed in (12) and briefly summarized as follows. We measured line tension over a range of temperatures *below* T_c by analyzing the power spectrum of domain boundary fluctuations. We measured correlation length over a range of temperatures *above* T_c by analyzing the structure factors of the fluorescent probe intensity. Correlation lengths are plotted in Figure 6. We fit experimental values of correlation lengths and line tensions for several vesicles and found $\nu = 1.2 \pm 0.2$, within error of the expected value of $\nu = 1$. We also measured β, the critical exponent for order parameter, and found $\beta = 0.124 \pm 0.03$, very close to the predicted value of $\beta = 0.125$. In the same set of experiments, we demonstrated that the membrane's critical exponent for compressibility, γ, is consistent with the 2-D Ising model prediction of 7/4. None of the values above are consistent with the critical exponents applicable either to the 3-D Ising model ($\nu = 0.630$ and $\beta = 0.325$) or to mean field theory ($\nu = 0.5$ and $\beta = 0.5$) (26). We concluded that lipid membranes faithfully exhibit critical behavior consistent with the universality class of the 2-D Ising model, and not with that either of the 3-D Ising model or of mean field theory (12).

There are several reasons why multi-component lipid bilayers are beautiful experimental systems for studying critical behavior in two dimensions.

1. Many phase diagrams have already been solved, and critical compositions and temperatures have been identified.
2. The critical temperature, T_c, is near room temperature (~300K), which simplifies experiments and makes it possible to probe small changes in reduced temperature $(T-T_c)/T_c$ without sophisticated temperature control.
3. Correlation lengths, ξ, are large and easy to optically resolve. Large correlation lengths are partly a result of a high critical temperature, T_c, and a concomitant small reduced temperature $(T-T_c)/T_c$. However, a high critical temperature is not sufficient to explain the exceptionally wide range of temperatures (10–15°C) over which we observe critical phenomena in membranes compared to other systems (e.g. (34)). We require ξ_0 to be large as well. Luckily, lipids are relatively large molecules (~1nm), meaning that ξ_0 and therefore ξ is large. Inserting experimental values into equation 3, we expect to find correlation lengths of >1μm for temperatures within ~0.5°C of the critical temperature, consistent with our experimental observations in Figure 6.
4. Lipid dynamics are fast enough for membranes to equilibrate quickly after changes in temperature, but slow enough that critical fluctuations are long lived, and can be visualized without the need for high speed data acquisition, as is often required to examine the dynamics of three dimensional binary liquids (e.g. (35)).

Ironically, our success in fitting membrane composition fluctuations to the 2-D Ising model over a broad range of temperatures has been bittersweet. We were happy to discover that lipid membranes near critical points are well modeled by considering only nearest-neighbor interactions. Moreover, we found it intriguing to contemplate what happens in membranes at higher temperatures, where we expect to find that membrane fluctuations persist below optical resolution, in accordance with equation 3. We can test this expectation by probing submicron length scales using experimental techniques such as nuclear magnetic resonance, which finds broadening of resonance peaks for membranes near critical points (9). On the

other hand, our happiness was mitigated because, as a result of being able to fit membrane fluctuations to the 2-D Ising model, we learned nothing new about the chemistry underlying the nearest-neighbor interactions between lipids (36). We have been thus unable to comment on whether phase separation in membranes is best described by models invoking lipid complexes (37), lipid chain order (38), the umbrella model (39), or any other molecular interactions.

ALTERNATE THEORIES OF SUBMICRON ORGANIZATION IN MEMBRANES

Our previous work demonstrates that composition fluctuations in lipid membranes scale in a manner consistent with the 2-D Ising model. Of course, critical fluctuations are not the only form in which small-scale regions of different composition can arise in lipid membranes. For example, given the right circumstances, membranes could constitute a 2-D microemulsion (40). In principle, different scenarios of membrane heterogeneity are straightforward to verify or refute quantitatively since they predict testable structure factors and/or critical exponents.

1. Microemulsions

The most common example of a 3-D emulsion is milk. The droplets contain oil and remain suspended in an aqueous phase because they are coated with surfactant. Milk appears white because it contains micron-scale droplets that scatter light. A microemulsion differs from an emulsion in that it forms spontaneously, is in equilibrium, and contains small, sub-micron droplets. High fractions of surfactant are required to coat the extensive interfacial surface of a microemulsion. The single thermodynamic phase of a microemulsion can exist alone, or can coexist with other phases (41). Addition of surfactant beyond the amount required for a single microemulsion phase eventually results in a lamellar phase with alternating sheets of oil and water coated with surfactant (42).

Given sufficient resolution, it is straightforward to determine if a lipid membrane constitutes a 2-D microemulsion. The spatial distribution of a microemulsion yields an oscillating autocorrelation function (41; 42) of the form

$$G(r) \propto e^{(-r/\xi)} \sin\left(\frac{2\pi r}{d} + \varphi\right). \quad [5]$$

This function captures the experimental signature of a microemulsion: short range order and long range disorder. In other words, the autocorrelation contains two length scales, a short distance (d) corresponding to the characteristic spacing of microemulsion droplets and a long distance (ξ) over which order decays. The simultaneous oscillation and decay are clear in figure 7. Gompper and Schick (42) assert that microemulsions are defined by the presence of a peak in the structure factor at the wavenumber, k, which is related to the droplet spacing, and that this peak distinguishes a microemulsion from a disordered fluid (41).

Under special circumstances, large scale emulsions can exhibit peaks in the structure factor, just as microemulsions do. In this case, the emulsion must be fractionally crystallized to yield monodisperse droplets, and attractive interactions between droplets must be invoked, as in depletion-attraction(43). These circumstances seem unlikely to be applicable to lipid membrane systems.

If a microemulsion contains very small domains, then the peak in $S(k)$ may occur at a wavenumber k that is not accessible by experiment. Nevertheless, it is still possible to

experimentally distinguish 2-D microemulsions from critical fluctuations because structure factors in the two systems differ substantially. Kotlarchyk and coworkers observed changes in the polydispersity of droplets in an oil-water microemulsion with varying temperature, and noted that the resulting structure factors were fit by assuming scattering from spherical droplets, not by assuming critical fluctuations (44).

In the very special case that a microemulsion's composition is manipulated so that a critical point is approached as temperature is varied, it is straightforward to experimentally assess the temperature regimes over which behavior relevant to either critical phenomena or microemulsions is relevant. At temperatures far from the critical point, structure factors derived from dynamic light scattering fit a form for individual droplets (45). Near the critical point, structure factors fit predictions relevant to critical fluctuations (45).

How much surfactant is required to create a 2-D microemulsion of droplets of radius a? If each surfactant molecule has a mean diameter l, then a ring of surfactant surrounding a 2-D droplet covers an area of approximately $(2\pi a)(l)$. The area of the circle inside the 2-D droplet is $\pi\,(a - l/2)^2$. For a worst-case estimate, assuming that the area outside the droplet is equal to the area inside, then the fraction of the total area covered by the surfactant ring is as follows:

$$\begin{aligned} surfactant\ area\ fraction &= \frac{area\ of\ ring}{area\ inside + outside\ the\ ring} \\ &= \frac{2\pi a l}{2\pi (a - l/2)^2} \\ &= \frac{1}{a} \quad for\ a \gg l \end{aligned} \qquad [6]$$

If each surfactant molecule covers approximately the area of one lipid, ~60Å^2, then l = 8.7Å (46). For a droplet of radius a = 26nm (as in (47)), the fraction of all area covered by surfactant is only ~5%. For a smaller droplet of radius a = 5nm, the surfactant area climbs to ~21%, a sizeable fraction of the membrane.

Which membrane components might function as surfactants in a 2-D microemulsion? In the absence of surfactant, the membrane contains two phases, one rich in lipids with high melting temperatures and the other rich in lipids with low melting temperatures. Saxton and Almeida have proposed that good candidates are lipids and proteins that have two faces with opposite binding tendencies (48). One such protein might be an N-Ras with one hexadecyl acyl chain and one farnesyl chain. This protein partitions primarily into the L_d phase, but in the minority of cases in which it is associated with the L_o phase, it tends to be located at the $L_d - L_o$ interface (49). Compelling examples of lipids with one saturated chain and one unsaturated chain include the common lipids POPC or SOPC (48). That said, it is worth noting that the hypothesis that POPC or SOPC functions as the surfactant in a 2-D microemulsion requires reconciling theoretical phase diagrams for emulsions (41; 42) with experimental phase diagrams in which POPC or SOPC is the main component of a macroscopic liquid disordered (50–52) or liquid ordered phase (53). This task is not necessarily impossible, but is certainly not trivial. Cholesterol is a similarly awkward candidate for a surfactant of a 2-D microemulsion since micron-scale domains appear in membranes containing cholesterol fractions of >50% (53). Moreover, adding cholesterol to a membrane can force lipids that were initially well mixed to macroscopically phase separate, which is diametrically opposite the role of a good surfactant (38). Experimentally, this is observed as a "closed-loop miscibility gap" such that increasing cholesterol concentration results in a lipid membrane that initially uniformly mixes, then phase separates, then uniformly mixes again (53).

2. Critical fluctuations with mean field exponents

Mean field theory assumes that each molecule in the system interacts with all others only in an average sense, through a field representing the equilibrium state of the overall system. This approximation means that correlations between fluctuations are not fully taken into account. Mean field theory produces critical exponents that are independent of the system's dimensionality. Exponents derived from mean field theory and from Ising model calculations yield the same critical exponents only when the system occupies ≥4 dimensions (54). As mentioned earlier, we have reported critical exponents in model lipid membranes to be $\nu = 1.2 \pm 0.2$ and $\beta = 0.124 \pm 0.03$ over a large range of temperatures (10–15°C) (12). These values are consistent with the exponents $\nu = 1$ and $\beta = 0.125$ within the 2-D Ising universality class, and not with the exponents $\nu = 0.5$ and $\beta = 0.5$ predicted by mean field theory.

Nevertheless, mean field theory is still applied to membranes near critical points. For example, rough agreement between mean field and Ising results have been used to argue that immobile, non-interacting obstacles embedded in membranes should have a strong effect on the membrane phase behavior and on the distribution of lipids over long length scales (55). Mean field calculations have also been used to make an order of magnitude estimate of the maximum correlation length with respect to the size of an individual lipid (56), and to estimate the decay rate of the time-correlation function of concentration fluctuations, a dynamic value that is difficult to find through full simulations (57). It is expected that mean field critical exponents will accurately describe fluctuations in membranes that are sufficiently far from the critical point in composition and/or temperature.

3. Nanodomains or microdomains

Recently, we (58) and others (59–65) have speculated that model membranes in equilibrium can contain 'nanodomains' or 'microdomains' of one liquid phase (e.g. liquid ordered) within another (e.g. liquid disordered). Researchers frequently hypothesize that nanodomains exist when membrane inhomogeneity is not resolvable as distinct, macroscopic phases. The range of nanodomain sizes plausible in each experiment depends on the experimental technique used. For example, the two techniques of fluorescence microscopy and NMR typically constrain nanodomains to be smaller than ~1μm and ~100nm, respectively (58; 63). Normally, in phase separated membranes at equilibrium, domains diffuse through the membrane, collide with other domains, and coalesce until only two large domains remain (51). In a scenario in which membrane nanodomains are distinct either from critical fluctuations or from 2-D microemulsions, it is postulated that domains nucleate, but that they aggregate or grow only until they reach sub-micron dimensions. In our own case, our speculation that microdomains existed eventually proved false (9).

To avoid growing larger, domains in a membrane either must not encounter each other through diffusion, or they must repel each other when they meet. Diffusion of membrane domains is indeed hindered when the membrane is close to a solid support, simply due to hydrodynamic considerations (66–68). However, solid supports are not employed in most experiments. Domain repulsion could take many forms, one of which is electrostatic (69). A different type of repulsion occurs when membranes within domains have a different curvature from the rest of the membrane (51; 70; 71). In many experimental systems in which membrane domains remain small, the system is kinetically trapped and is not in its overall lowest energy state. Whatever the source of the repulsion, it must vary with composition and temperature in such a way to explain why researchers reporting nanodomains in some lipid membranes also observe large, experimentally resolvable domains in membranes of similar lipid composition, or in the same lipid membrane at lower

temperatures. Moreover, if domains remain small due to kinetic processes, then hysteresis should be observed as temperature is cycled through the transition.

As we have discussed in previous sections, composition fluctuations in membranes above a critical temperature can have sub-micron correlation lengths. In our own experiments, we were able to justify our deuterium NMR data well by considering membrane critical fluctuations and a shift in the transition temperature (9; 72), which alleviated our need to speculate that sub-micron domains existed (51). It seems plausible that further investigation of some of the systems in which nanodomains have been proposed may eventually yield evidence for either membrane critical fluctuations or microemulsions.

Nanodomains of the type postulated by Frolov et al. are predicted to appear when line tension is lowered sufficiently (e.g. <0.18pN) (73). In fluorescence microscopy experiments, low line tension is not a sufficient condition for the formation of nanodomains because micron-scale, phase separated domains are observed even when measured line tensions approach zero (e.g. well below 0.1pN), as occurs near critical points (10–12). Nevertheless, it is worth noting that the theory of Frolov et al. is testable. The authors interpret their results as predicting “a monodisperse ensemble of *n* small domains,” which suggests a structure factor similar to that of a microemulsion. In principle, experiments can be designed to distinguish the theory proposed by Frolov et al. and other possible theories of submicron organization with distinct structure factors, such as membrane critical fluctuations.

4. Non-ideal mixing

In its most general usage, the term “non-ideal mixing” encompasses all deviations from random distributions exhibited in ideal gases or solutions, independent of mechanism. Traditionally, non-ideal mixtures have been experimentally identified by non-zero enthalpies of mixing or by deviations from Raoult’s Law (as in the azeotrope of water and ethanol). In simple lipid mixtures, non-ideal mixing manifests itself in phase diagrams and specific heats that deviate from those expected for systems that mix ideally (74–79). Phase separation is typically not considered non-ideal mixing, but rather as ideal mixing in two separate phases.

In statistical mechanics, correlations or inhomogeneities that extend beyond a few molecular diameters in space or beyond a few relaxation times demand a physical explanation. There are many possible configurations of molecules that result in non-ideal mixing on long time and distance scales, including microemulsions, critical fluctuations, and templating by substrates. For the cases of critical fluctuations and microemulsions, it is possible to distinguish these two types of non-ideal mixing by comparing correlation functions as in figures 3 and 7, as described earlier.

IMMISCIBILITY AND FLUCTUATIONS IN BIOMEMBRANES

Our studies of model membranes are motivated in part by our interest in the physical interactions that give rise to lateral heterogeneity in cell plasma membranes. However, the task of predicting the phase behavior of cell membranes is intractably complex. Unlike simple model membranes, cell membranes contain hundreds to thousands of different lipid species and a high density of membrane-bound proteins (80; 81). In addition, the plasma membrane is connected to the cell interior through cytoskeletal components, and through trafficking of membrane lipids and proteins to and from the cell surface. In order to apply any results from model membranes to cells, it is important that we investigate properties of membranes that do not depend on the details of the system. Critical point behavior is an example of a property that can be fruitfully investigated in complex biophysical systems.

1. Observations of critical fluctuations in plasma membrane vesicles

Giant plasma membrane vesicles (GPMVs) are spherical vesicles isolated directly from the plasma membranes of living cells (82). They retain much of the compositional complexity of the intact cell plasma membrane, but lack cytoskeletal components (82; 83) and may possess different lipid compositions. Membranes of GPMVs demix into coexisting liquid ordered and liquid disordered phases at low temperature (84), and protein and lipid components partition unequally into the two phases (84; 85). Remarkably, GPMVs undergo robust critical fluctuations when temperature is held near the transition temperature as shown in figure 8 (11).

Analysis of structure factors of images similar to those in figure 8 illustrate that GPMV membranes have critical compositions, and that these complex biomembranes pass through a critical point at the transition temperature of roughly room temperature. While it is not surprising that critical fluctuations appear in the simple model membranes described in previous sections, which were specially prepared to pass through a critical point at the transition temperature, it is remarkable that the same robust critical behavior occurs in the complex lipid and protein compositions of GPMV membranes. Just as in model membranes, fluctuations in GPMVs conform to scaling laws associated with the 2-D Ising universality class (11). Measured line tensions and correlation lengths in GPMVs superimpose beautifully on the same values from model membranes, as shown in Figure 6. These results indicate that, despite the complexity of GPMVs, composition fluctuations in GPMVs can be fit to a simple model of up and down spins on a two dimensional lattice.

The discovery of robust critical behavior in plasma membrane vesicles raises two questions regarding critical points in complex membranes.

1. ‘Does a large number of lipid types make it easier to land on a critical point at any arbitrary composition and temperature?’ The answer is no. Thermodynamic rules govern the space of possible critical points for a system at fixed pressure. A two-component mixture has a maximum of one upper consolute critical point. A three-component mixture can have a line of critical points. A four component mixture can have a surface of critical points, and so on. Although complex mixtures with more components can contain more critical points, those points are no easier (and no more difficult) to encounter while randomly searching through compositions and temperatures than in a system with fewer components.
2. ‘Does a large number of lipid types make it easier to move to a critical point from any arbitrary composition and temperature?’ The answer is yes. Since complex systems have more critical points, a cell whose membrane has more lipid types has more flexibility in how to adjust lipid compositions in order to move to one of the many possible critical points. For example, if the cell is not able to change the membrane composition of one type of lipid or protein, it can adjust another in order to move to a critical point. Indeed, a wide range of critical temperatures are found in GPMVs isolated from distinct cells, indicating that individual GPMVs have compositions corresponding to different critical points (11).

2. Predictions and Implications

Observations of critical fluctuations in plasma membrane vesicles indicate that cell plasma membranes, as represented by GPMVs, have critical compositions. The relative rarity of critical points amongst all possible lipid compositions, even in complex mixtures, suggests that cells must actively regulate membrane composition to maintain proximity to a critical point. How might a cell take advantage of critical behavior in its plasma membrane? We can use the principles of universality to generate a few predictions.

First, we predict that submicron critical fluctuations are present in GPMV membranes at physiological temperatures. Since critical temperatures measured in GPMVs generally fall at or below room temperature, large, micron-scale critical fluctuations occur in GPMV membranes only at temperatures well below normal physiological temperatures of 37°C. Since critical fluctuations in GPMVs conform to the 2D Ising universality class, we can extrapolate using equation 3 to predict that GPMVs like those shown in figure 8 contain critical fluctuations with a correlation length of ~20 nm at 37°C. If the compositions of cell plasma membranes are well represented in isolated GPMVs, then we also expect to find composition fluctuations with correlation lengths ~20 nm in the plasma membranes of intact cells at their growth temperature of 37°C. It is tempting to speculate that critical fluctuations form the physical basis of at least some of the membrane inhomogeneity attributed to 'rafts' in cell membranes. Currently, one of us (SLV) is testing this hypothesis by comparing correlation functions and structure factors predicted by critical phenomena with distributions of proteins and lipids on the cell surface using experimental techniques sensitive to nanometer-scale organization.

Second, we expect that many factors will modulate the size and stability of regions of compositional heterogeneity in GPMVs (and presumably also in cell membranes). In the model membrane and GPMV experiments described here, correlation lengths, ξ, are tuned by changing temperature, as in figure 9a. In cell membranes, which function at constant temperature, correlation lengths could be controlled by changing composition of the membrane in order to alter the critical temperature or composition as in figure 9c (86). It is now well established that small changes in membrane composition or structure can produce large changes in miscibility transition temperatures in model membranes (72; 87–90). It is possible that cells have developed similar mechanisms to modulate critical temperatures in their plasma membranes.

We can entertain additional speculations – some of which we have detailed previously (86) – based on the observations that GPMV and model membranes with critical compositions exhibit dynamic composition fluctuations driven by thermal energy (kT). In this regime, the energy associated with assembling components is low, and cells could plausibly supply the energy to augment the assembly of membrane components though active processes involving membrane proteins, or direct binding of membrane components. If a membrane is poised close enough to a critical point, the slow mixing dynamics associated with critical systems (26) may increase the lifetime and functional consequences of active associations. Objects outside the membrane plane may also influence fluctuation dynamics (56). Moreover, the fascinating wetting behavior that occurs near critical points (91) may promote protein clustering (92; 93) in a manner similar to the shell hypothesis (94).

3. Cytoskeleton, Asymmetry, and Recycling

Although GPMVs retain much of the compositional complexity of cell plasma membranes, they do not capture other important aspects of intact cells that need to be explored in future studies. For example, crosslinking can perturb miscibility phase boundaries (87), and GPMVs are typically isolated from cells treated by a mild crosslinking agent. It is also important to note that GPMVs do not contain cytoskeletal components, which are thought to play an important role in the assembly of 'raft' domains in cells and in the diffusion of membrane components across the cell surface (95; 96). Studies in model membranes have shown that the presence of cytoskeletal proteins can alter phase boundaries (88). Moreover, lipids in membranes in contact with intact cytoskeletons may experience slow collective motion as in membranes near solid supports (66; 67). Another topic to consider is that the cell's plasma membrane composition is in constant flux (97–100). Last, cell plasma membranes are asymmetric (101) and some asymmetry is likely lost during GPMV formation (84). Coupling between the two leaflets of an asymmetric bilayer membrane has

been experimentally shown to result in the induction of domains from one leaflet to the other (or the annihilation of domains in both leaflets)(102), which will certainly change the location of critical points (103–105). None of the aspects above necessarily detracts from the speculation that cell membranes may be poised near critical points, but they do significantly add to the challenge of predicting the composition, temperature, and other experimental conditions under which critical behavior might be observed in cell systems.

4. Proposed Microemulsions in Cell Membranes

Microemulsions have been suggested as a way to achieve sub-micron lateral inhomogeneity in cell membranes (10; 40; 48). Since experiments with GPMV's imply that cell membranes have compositions near critical points (11), which creates sub-micron lateral inhomogeneity, it is unnecessary to invoke microemulsions.

Of course, the experimental observation of critical fluctuations in GPMVs does not disprove the hypothesis that cell membranes contain microemulsions. The hypothesis can be directly tested using equation 5. What would be required for a membrane to contain a microemulsion? If we require the membrane microemulsion to contain 2-D droplets within a narrow size range, then our estimate in equation 6 for the fraction of all membrane area covered by surfactants in a microemulsion tells us that lipid and protein compositions must be stringently regulated. It has been proposed that minority lipids or proteins could play the role of the surfactant between phases in a lipid membrane (40). Using our worst-case estimate, this proposal is feasible for 2-D droplets of ~50nm (40), whereas smaller droplets of ~10nm would require significant surfactant concentrations. Overshooting this concentration should result in a 2-D lamellar phase (42).

It is worth noting that the set of experimental conditions resulting in a microemulsion is small. The set of conditions resulting in critical point behavior is also small. The intersection between the two sets is even smaller. Simultaneously requiring that a plasma membrane of a resting cell is equivalent to a 2-D microemulsion and that membranes of GPMVs made from the same cell are near a critical point places very strong constraints on the system. In microemulsions, small droplets persist to low temperatures. In contrast, in plasma membrane vesicles, the membrane is poised above a critical point at the growth temperature, and domains grow large at lower temperatures. To achieve both conditions, the process of forming plasma membrane vesicles must selectively exclude certain lipids and proteins acting as a surfactant in the microemulsion of the original cell membrane. We know that some selection of membrane components does indeed occur (82). In the microemulsion scenario, this selection must be exquisitely controlled because although addition of surfactant to a range of phase-separated systems results in microemulsions, the opposite process, removal of surfactant from a microemulsion, is unlikely to leave the system poised above a critical point. The microemulsion scenario becomes more unlikely in light of the variety of experimental conditions under which critical fluctuations are observed in GPMVs (11). Of course, "unlikely" is not the same as "impossible".

To review our discussion above, there exist three solid experimental tests of whether a cell membrane contains a microemulsion. First, the autocorrelation function of lipids and proteins distributed across the cell surface should display a peak at nonzero k as in equation 5. Second, the process of forming a plasma membrane vesicle should leave the cell membrane with a higher concentration of surfactant, which might result in a 2-D lamellar phase (42). Third, this same lamellar phase should be experimentally accessible through over-expression of whatever molecule behaves as the 2-D surfactant. To our knowledge, an experimental strategy to test these predictions has not been pursued to date.

CONCLUSION

Part of the interest and challenge in studying biological systems lies in their complexity. This complexity can quickly become overwhelming after only cursory investigation, such as a glance at a chart of biochemical pathways. For a system poised near a critical point, much of the observable behavior simplifies and is described by universal scaling laws. Remarkably, it is not difficult to find critical behavior in compositionally complex lipid membranes, even ones derived from living cell membranes. We find that membranes produced both of ternary mixtures of lipids and of plasma membrane vesicles contain composition fluctuations well described by the 2-D Ising model for critical phenomena. Critical fluctuations are distinguished from microemulsions and other forms of non-ideal mixing by well-defined properties that can be evaluated experimentally. By applying principles of universality, it is possible to quantitatively characterize lateral heterogeneity in systems near critical points, even in complex biomembranes.

Acknowledgments

We thank the editors of this issue for the invitation to submit this review article. We thank Barbara Baird, David Holowka, Harden McConnell, Jim Sethna, Michael Schick, and Ben Widom for helpful discussions. We are grateful to Marcus Collins for Ising model simulations. We separately thank Jake Ashcraft, Ethan Chiang, Marcus Collins, Tony Dinsmore, Fred Heberle, Thalia Mills, Greg Garbes Putzel, Michael Schick, Jim Sethna, and Norah Smith for thoughtful comments on various sections and drafts of our manuscript. Responsibility for any remaining errors or lack of clarity rests on our shoulders alone. ARHS is supported by a UW Molecular Biophysics Training grant NIH #5 T32 GM08268-20. SLV is supported through the Irvington Institute Fellowship Program of the Cancer Research Institute and the William T. Miller Independent Scientist Program at Cornell University. SLK acknowledges support from the National Science Foundation MCB-0744852.

References

1. Weisenfeld K. Resource Letter: ScL-1: Scaling Laws. Am J Phys. 2001; 69:938–942.
2. Liu Y, Dilger JP. Application of the one- and two-dimensional Ising models to studies of cooperativity between ion channels. Biophys J. 1993; 64:26–35. [PubMed: 7679298]
3. Schneidman E, Berry MJ II, Segev R, Bialek W. Weak pairwise correlations imply strongly correlated network states in a neural population. Nature. 2006; 440:1007–1012. [PubMed: 16625187]
4. Wetzel SK, Settanni G, Kenig M, Binz HK, Plückthun A. Folding and unfolding mechanism of highly stable full-consensus ankyrin repeat proteins. J Mol Biol. 2008; 376:241–257. [PubMed: 18164721]
5. Cellmer T, Henry ER, Kubelka J, Hofrichter J, Eaton WA. Relaxation rate for an ultrafast folding protein is independent of chemical denaturant concentration. J Am Chem Soc. 2007; 129:14564–14565. [PubMed: 17983235]
6. Liu H, Kumar SK, Sciortino F. Vapor-liquid coexistence of patchy models: Relevance to protein phase behavior. J Chem Phys. 2007; 127:084902–084901–084902–084905. [PubMed: 17764289]
7. Rice PA, McConnell HM. Critical shape transitions of monolayer lipid domains. Proc Natl Acad Sci USA. 1989; 86:6445–6448. [PubMed: 16594064]
8. Keller SL, McConnell HM. Stripe phases in lipid monolayers near a miscibility critical point. Phys Rev Lett. 1999; 82:1602–1605.
9. Veatch SL, Soubias O, Keller SL, Gawrisch K. Critical fluctuations in domain-forming lipid mixtures. Proc Natl Acad Sci USA. 2007; 104:17650–17655. [PubMed: 17962417]
10. Esposito C, Tian A, Melamed S, Johnson C, Tee SY, Baumgart T. Flicker spectroscopy of thermal lipid bilayer domain boundary fluctuations. Biophys J. 2007; 93:3169–3181. [PubMed: 17644560]
11. Veatch SL, Cicuta P, Sengupta P, Honerkamp-Smith A, Holowka D, Baird B. Critical fluctuations in plasma membrane vesicles. ACS Chem Biol. 2008; 3:287–293. [PubMed: 18484709]

12. Honerkamp-Smith A, Cicuta P, Collins MD, Veatch SL, den Nijs M, Schick M, Keller SL. Line tensions, correlation lengths, and critical exponents in lipid membranes near critical points. Biophys J. 2008; 95:236–246. [PubMed: 18424504]
13. Baake E, Baake M, Wagner H. Ising quantum chain is equivalent to a model fo biological evolution. Phys Rev Lett. 1997; 78:559–562.
14. Leuthäusser I. An exact correspondence between Eigen's evolution model and a two-dimensional Ising system. J Chem Phys. 1986; 84:1884–1885.
15. Woloszyn M, Stauffer D, Kulakowski K. Order-disorder phase transition in a cliquey social network. Eur Phys J B. 2007; 57:331–335.
16. Totafurno J, Lumsden CJ, Trainor LEH. Structure and function in biological hierarchies: An Ising model approach. J Theor Biol. 1980; 85:171–198. [PubMed: 7431953]
17. Fisher ME. Correlation functions and the critical region of simple fluids. J Math Phys. 1964; 5:944–962.
18. Fisher ME. The theory of equilibrium critical phenomena. Rep Prog Phys. 1967; 30:615–730.
19. Guyon E. Second-order phase transitions: Models and analogies. Am J Phys. 1975; 43:877–881.
20. Mowery AC, Jacobs DT. Undergraduate experiment in critical phenomena: Light scattering in a binary fluid mixture. Am J Phys. 1983; 51:542–545.
21. Sengers JV, Levelt Sengers JMH. Thermodynamic behavior of fluids near the critical point. Ann Rev Phys Chem. 1986; 37:189–222.
22. Mayorga A, Thompson D. A critical exponent of an aniseed-based liquor. Am J Phys. 1996; 64:621–623.
23. Tobochnik J. Resource letter CPPPT-1: Critical point phenomena and phase transitions. Am J Phys. 2001; 69:255–263.
24. Stanley, HE. Introduction to phase transitions and critical phenomena. Oxford University Press; New York: 1971.
25. Rowlinson, JS.; Widom, B. The molecular theory of capillarity. Clarendon Press; Oxford: 1982.
26. Goldenfeld, N. Lectures on phase transitions and the renormalization group. Addison-Wesley; New York: 1992.
27. Onsager L. Crystal statistics. I. A two-dimensional model with an order-disorder transition. Phys Rev. 1944; 65:117–149.
28. Itzykson, C.; Drouffe, J-M. Statistical Field Theory. Vol. 1. Cambridge University Press; New York: 1992.
29. Wilson KG. Problems in physics with many scales of length. Scientific American. 1971; 241:158–179.
30. Maris HJ, Kadanoff LP. Teaching the renormalization group. Am J Phys. 1978; 46:652–657.
31. Bruce, A.; Wallace, D. Critical point phenomena: universal physics at large length scales. In: Davies, PCW., editor. The New Physics. Cambridge University Press; New York: 1989.
32. Stanley HE. Scaling, universality, and renormalization: Three pillars of modern critical phenomena. Rev Mod Phys. 1999; 71:S358–S366.
33. Kaufman B, Onsager L. Crystal statistics. III. Short-range order in a binary Ising lattice. Phys Rev. 1949; 76:1244–1252.
34. Schwahn D, Mortensen K, Yee-Madeira H. Mean-field and Ising critical behavior of a polymer blend. Phys Rev Lett. 1987; 58:1544–1546. [PubMed: 10034466]
35. Kostko AF, Anisimov MA, Sengers JV. Dynamics of critical fluctuations in polymer solutions. Phys Rev E. 2007; 76:021804.
36. McConnell HM. Understanding membranes. ACS Chem Biol. 2008; 3:265–267. [PubMed: 18484706]
37. Radhakrishnan A, McConnell HM. Composition fluctuations, chemical exchange, and nuclear relaxation in membranes containing cholesterol. J Chem Phys. 2007; 126:185101–185101–185101–185111. [PubMed: 17508832]
38. Garbes Putzel G, Schick M. Phenomenological model and phase behavior of saturated and unsaturated lipids and cholesterol. Biophys J. 2008 in press.

39. Huang JY, Feigenson GW. A microscopic interaction model of maximum solubility of cholesterol in lipid bilayers. Biophys J. 1999; 76:2142–2157. [PubMed: 10096908]
40. Simons K, Vaz WLC. Model systems, lipid rafts, and cell membranes. Annu Rev Biophys Biomol Struct. 2004; 33:269–295. [PubMed: 15139814]
41. Gompper G, Schick M. Lattice model of microemulsions: the effect of fluctuations in one and two dimensions. Phys Rev A. 1990; 42:2137–2149. [PubMed: 9904262]
42. Gompper G, Schick M. Lattice model of microemulsions. Phys Rev B. 1990; 41:9148–9162.
43. Bibette J, Roux D, Nallet F. Depletion interactions and fluid-solid equilibrium in emulsions. Phys Rev Lett. 1990; 65:2470–2473. [PubMed: 10042556]
44. Kotlarchyk M, Chen SH, Huang JS. Temperature dependence of size and polydispersity in a three-component microemulsion by small-angle neutron scattering. J Phys Chem. 1982; 86:3273–3276.
45. Rouch J, Safouane A, Tartaglia P, Chen SH. Experimental evidence of a crossover in critical behaviour of water-in-oil emulsions. J Phys: Condens Matter. 1989; 1:1773–1778.
46. Nagle JF. Area/lipid of bilayers from NMR. Biophys J. 1993; 64:1476–1481. [PubMed: 8324184]
47. Pralle A, Keller P, Florin EL, Hörber JKH. Sphingolipid-cholesterol rafts diffuse as small entities in the plasma membrane of mammalian cells. J Cell Biol. 2000; 148:997–1007. [PubMed: 10704449]
48. Saxton M, Oldham A, Almeida P. Two-dimensional detergents and lipid raft organization. Biophys J. 2005; 88:412A–412A. [PubMed: 15475587]
49. Nicolini C, Baranski J, Schlummer S, Palomo J, Lumbierres-Burgues M, Kahms M, Kuhlmann J, Sanchez S, Gratton E, Waldmann H, Winter R. Visualizing association of N-Ras in lipid microdomains: Influence of domain structure and interfacial adsorption. J Am Chem Soc. 2006; 126:192–201. [PubMed: 16390147]
50. Veatch SL, Keller SL. Miscibility phase diagrams of giant vesicles containing sphingomyelin. Phys Rev Lett. 2005; 94:148101–148101–148101–148104. [PubMed: 15904115]
51. Veatch SL, Keller SL. Separation of liquid phases in giant vesicles of ternary mixtures of phospholipids and cholesterol. Biophys J. 2003; 85:3074–3083. [PubMed: 14581208]
52. Garg S, Ruhe J, Ludtke K, Jordan R, Naumann CA. Domain registration in raft-mimicking lipid mixtures studied using polymer-tethered lipid bilayers. Biophys J. 2007; 92:1263–1270. [PubMed: 17114215]
53. Veatch SL, Gawrisch K, Keller SL. Closed-loop miscibility gap and quantitative tie-lines in ternary membranes containing diphytanoyl PC. Biophys J. 2006; 90:4428–4436. [PubMed: 16565062]
54. Als-Nielsen J, Birgeneau RJ. Mean field theory, the Ginzburg Criterion, and marginal dimensionality of phase transitions. Am J Phys. 1977; 45:554–560.
55. Yethiraj A, Weisshaar JC. Why are lipid rafts not observed in vivo? Biophys J. 2007; 93:3113–3119. [PubMed: 17660324]
56. Tserkovnyak Y, Nelson DR. Conditions for extreme sensitivity of protein diffusion in membranes to cell environments. Proc Natl Acad Sci USA. 2006; 103:15002–15007. [PubMed: 17008402]
57. Seki K, Komura S, Imai M. Concentration fluctuations in binary fluid membranes. J Phys: Condens Matter. 2007; 19:072101–072101–072101–072108.
58. Veatch SL I, Polozov V, Gawrisch K, Keller SL. Liquid domains in vesicles investigated by NMR and fluorescence microscopy. Biophys J. 2004; 86:2910–2922. [PubMed: 15111407]
59. Feigenson GW, Buboltz JT. Ternary phase diagram of dipalmitoyl-PC/dilauroyl-PC/cholesterol: nanoscopic domain formation driven by cholesterol. Biophys J. 2001; 80:2775–2788. [PubMed: 11371452]
60. Silvius JR. Fluorescence energy transfer reveals microdomain formation at physiological temperatures in lipid mixtures modeling the outer leaflet of the plasma membrane. Biophys J. 2003; 85:1034–1045. [PubMed: 12885650]
61. Silvius J. Lipid microdomains in model and biological membranes: how strong are the connections? Quarterly Reviews of Biophysics. 2005; 38:373–383. [PubMed: 16600056]
62. Feigenson G. Phase boundaries and biological membranes. Annu Rev Biophys Biomol Struct. 2007; 36:63–77. [PubMed: 17201675]

63. Bunge A, Müller P, Stöckl M, Herrmann A, Huster D. Characterization of the ternary mixture of sphingomyelin, POPC, and cholesterol: Support for an inhomogeneous lipid distribution at high temperatures. Biophys J. 2008; 94:2680–2690. [PubMed: 18178660]
64. Krivanek R, Okoro L, Winter R. Effect of cholesterol and ergosterol on the compressibility and volume fluctuations of phospholipid-sterol bilayers in the critical point region: A molecular acoustic and calorimetric study. Biophys J. 2008; 94:3538–3548. [PubMed: 18199673]
65. Soni SP, LoCascio DS, Liu Y, Williams JA, Bittman R, Stillwell W, Wassall SR. Docosahexanoic acid enhances segregation of lipids between raft and nonraft domains: 2H-NMR study. Biophys J. 2008; 95:203–214. [PubMed: 18339742]
66. Stottrup BL, Veatch SL, Keller SL. Nonequilibrium behavior in supported lipid membranes containing cholesterol. Biophys J. 2004; 86:2942–2950. [PubMed: 15111410]
67. Kaizuka Y, Groves JT. Structure and dynamics of supported intermembrane junctions. Biophys J. 2004; 86:905–912. [PubMed: 14747326]
68. Stone HA, Ajdari A. Hydrodynamics of particles embedded in a flat surfactant layer overlying a subphase of finite depth. J Fluid Mech. 1998; 369:151–173.
69. Liu J, Qi S, Groves JT, Chakraborty AK. Phase segregation on different length scales in a model cell membrane system. J Phys Chem. 2005; 109:19960–19969.
70. Rozovsky S, Kaizuka Y, Groves JT. Formation and spatio-temporal evolution of periodic structures in lipid bilayers. J Am Chem Soc. 2005; 127:36–37. [PubMed: 15631436]
71. Baumgart T, Hess ST, Webb WW. Imaging coexisting fluid domains in biomembrane models coupling curvature and line tension. Nature. 2003; 425:821–824. [PubMed: 14574408]
72. Veatch SL, Leung SS, Hancock RE, Thewalt JL. Fluorescent probes alter miscibility phase boundaries in ternary vesicles. J Phys Chem. 2007; 111:502–504.
73. Frolov VAJ, Chizmadzhev YA, Cohen FS, Zimmerberg J. “Entropic traps” in the kinetics of phase separation in mulitcomponent membranes stabilize nanodomains. Biophys J. 2006; 91:189–205. [PubMed: 16617071]
74. Jørgensen K, Sperotto MM, Mouritsen OG, Ipsen JH, Zuckermann MJ. Phase equilibria and local structure in binary lipid bilayers. Biochim Biophys Acta. 1993; 1152:135–145. [PubMed: 8399291]
75. Huang J, Swanson JE, Dibble AR, Hinderliter AK, Feigenson GW. Nonideal mixing of phosphatidylserine and phosphatidylcholine in the fluid lamellar phase. Biophys J. 1993; 64:413–425. [PubMed: 8457667]
76. Garidel P, Johann C, Blume A. Nonideal mixing and phase separation in phosphatidylcholine-phosphatidic acid mixtures as a function of acyl chain length and pH. Biophys J. 1997; 71:2196–2210. [PubMed: 9129822]
77. Huster D, Arnold K, Gawrisch K. Influence of docosahexanoic acid and cholesterol on lateral lipid organization in phospholipid mixtures. Biochemistry. 1998; 37:17299–17308. [PubMed: 9860844]
78. Tokutake N, Jing B, Regen SL. Detection of unusual lipid mixing in cholesterol-rich phospholipid bilayers: The long and short of it. J Am Chem Soc. 2003; 125:8994–8995. [PubMed: 15369338]
79. McConnell HM, Vrljic M. Liquid-liquid immiscibility in membranes. Annu Rev Biophys Biomol Struct. 2003; 32:469–492. [PubMed: 12574063]
80. Myher JJ, Kuskis A, Pind S. Molecular species of glycerophospholipids and sphingomyelins of human erythrocytes: Improved method of analysis. Lipids. 1989; 24:396–407. [PubMed: 2755317]
81. van Meer G. Cellular lipidomics. EMBO Journal. 2005; 24:3159–3165. [PubMed: 16138081]
82. Holowka D, Baird B. Sturctural studies on the membrane-bound immunoglobulin E-receptor complex. 1. Characterization of large plasma membrane vesicles from rat basophilic leukemia cells and insertion of amphipathic fluorescent probes. Biochemistry. 1983; 22:3466–3474. [PubMed: 6225455]
83. Fridriksson EK, Shipkova PA, Sheets ED, Holowka D, Baird B, McLafferty FW. Quantitative analysis of phospholipids in functionally important membrane domains from RBL-2H3 mast cells using tandem high-resolution mass spectrometry. Biochemistry. 1999; 38:8056–8063. [PubMed: 10387050]

84. Baumgart T, Hammond AT, Sengupta P, Hess ST, Holowka DA, Baird BA, Webb WW. Large-scale fluid/fluid phase separation of proteins and lipids in giant plasma membrane vesicles. Proc Natl Acad Sci USA. 2007; 104:3165–3170. [PubMed: 17360623]
85. Sengupta P, Hammond A, Holowka D, Baird BA. Structural determinants for partitioning of lipids and proteins between coexisting fluid phases in giant plasma membrane vesicles. Biochim Biophys Acta. 2008; 1778:20–32. [PubMed: 17936718]
86. Veatch SL. From small fluctuations to large-scale phase separation: lateral organization in model membranes containing cholesterol. Semin Cell Dev Biol. 2007; 18:573–582. [PubMed: 17942350]
87. Hammond AT, Heberle FA, Baumgart T, Holowka D, Baird B, Feigenson GW. Crosslinking a lipid raft component triggers liquid ordered-liquid disordered phase separation in model plasma membranes. Proc Natl Acad Sci USA. 2005; 102:6320–6325. [PubMed: 15851688]
88. Liu AP, Fletcher DA. Actin polymerization serves as a membrane domain switch in model lipid bilayers. Biophys J. 2006; 91:4064–4070. [PubMed: 16963509]
89. Ayuyan AG, Cohen FS. Lipid peroxides promote large rafts: effects of excitation of probes in fluorescence microscopy and electrochemical reactions during vesicle formation. Biophys J. 2006; 91:2172–2183. [PubMed: 16815906]
90. Zhao J, Wu J, Shao H, Kong F, Jain N, Hunt G, Feigenson G. Phase studies of model biomembranes: macroscopic coexistence of Lalpha+Lbeta, with light induced coexistence of Lalpha+Lo phases. Biochim Biophys Acta. 2007; 1768:2777–2786. [PubMed: 17931595]
91. Cahn JW. Critical point wetting. J Chem Phys. 1977; 66:3667–3672.
92. Beysens D, Narayanan T. Wetting-induced aggregation of colloids. J Stat Phys. 1999; 95:997–1008.
93. Owicki JC, Springgate MW, McConnell HM. Theoretical study of protein-lipid interactions in bilayer membranes. Proc Natl Acad Sci USA. 1978; 75:1616–1619. [PubMed: 273895]
94. Anderson RG, Jacobson K. A role for lipid shells in targeting proteins to caveolae, rafts, and other lipid domains. Science. 2002; 296:1821–1825. [PubMed: 12052946]
95. Edidin M. Shrinking patches and slippery rafts: scales of domains in the plasma membrane. Trends in Cell Biol. 2001; 11:492–496. [PubMed: 11719055]
96. Suzuki K, Ritchie K, Kajikawa E, Fujiwara T, Kusumi A. Rapid hop diffusion of a G-protein-coupled receptor in the plasma membrane as revealed by single-molecule techniques. Biophys J. 2005; 88:3659–3680. [PubMed: 15681644]
97. Wustner D, Herrmann A, Hao M, Maxfield FR. Rapid nonvesicular transport of sterol between the plasma membrane domains of polarized hepatic cells. J Biol Chem. 2004; 277:30325–30336. [PubMed: 12050151]
98. Holthuis JC, Levine TP. Lipid traffic: floppy drives and a superhighway. Nat Rev Mol Cell Biol. 2005; 6:209–220. [PubMed: 15738987]
99. van Meer G. Lipid traffic in animal cells. Annu Rev Cell Biol. 1989; 5:247–275. [PubMed: 2688705]
100. Gheber LA, Edidin M. A model for membrane patchiness: lateral diffusion in the presence of barriers and vesicle traffic. Biophys J. 1999; 77:3163–3175. [PubMed: 10585938]
101. Bretscher MS. Asymmetrical lipid bilayer structure for biological membranes. Nature New Biol. 1972; 236:11–12. [PubMed: 4502419]
102. Collins MD, Keller SL. Tuning lipid composition to induce domains across leaflets of unsupported lipid bilayers. Proc Natl Acad Sci USA. 2007; 105:124–128. [PubMed: 18172219]
103. Allender DW, Schick M. Phase separation in bilayer membranes: effects on the inner leaf due to coupling to the outer leaf. Biophys J. 2006; 91:2928–2935. [PubMed: 16877505]
104. Wagner AJ, Loew S, May S. Influence of a monolayer-monolayer coupling on the phase behavior of a fluid lipid bilayer. Biophys J. 2007; 93:4268–4277. [PubMed: 17766349]
105. Garbes Putzel G, Schick M. Phase behavior of a model bilayer membrane with coupled leaves. Biophys J. 2008; 94:869–877. [PubMed: 17905845]
106. Hohenberg PC, Halperin BI. Theory of dynamic critical phenomena. Rev Mod Phys. 1977; 49:435–479.

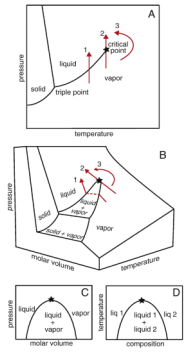

Figure 1.

(A) Phase diagram for water in the pressure-temperature plane. Path 1 crosses a coexistence line at which the vapor becomes a liquid. Along path 2, the same transition occurs at a critical point, which is marked with a star. Path 3 follows a continuous change from vapor to liquid without crossing the coexistence line. (B) The same paths are shown on a 3-dimensional phase diagram. (C) When molar volume is considered, there is a region of vapor and liquid coexistence, rather than merely a line. This region ends in a critical point. (D) The same type of phase diagram describes miscibility of two liquids, where the critical point is an upper consolute point.

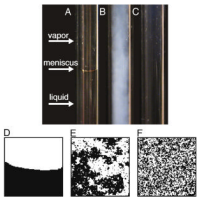

Figure 2.

(A) At room temperature, a glass tube filled with pressurized carbon dioxide contains liquid CO_2 and vapor. A meniscus is clearly visible. Only the interior of the tube is shown. (B) The meniscus disappears when temperature is raised to the critical point. The observed cloudiness results from critical opalescence. (C) Above the critical temperature, the entire tube is filled with a single fluid phase. (D–F) The same behavior is captured by a simulation of the two-dimensional Ising model conducted far below (D), at (E), and far above (F) its critical temperature. The simulation was conducted as in (12) by Marcus Collins.

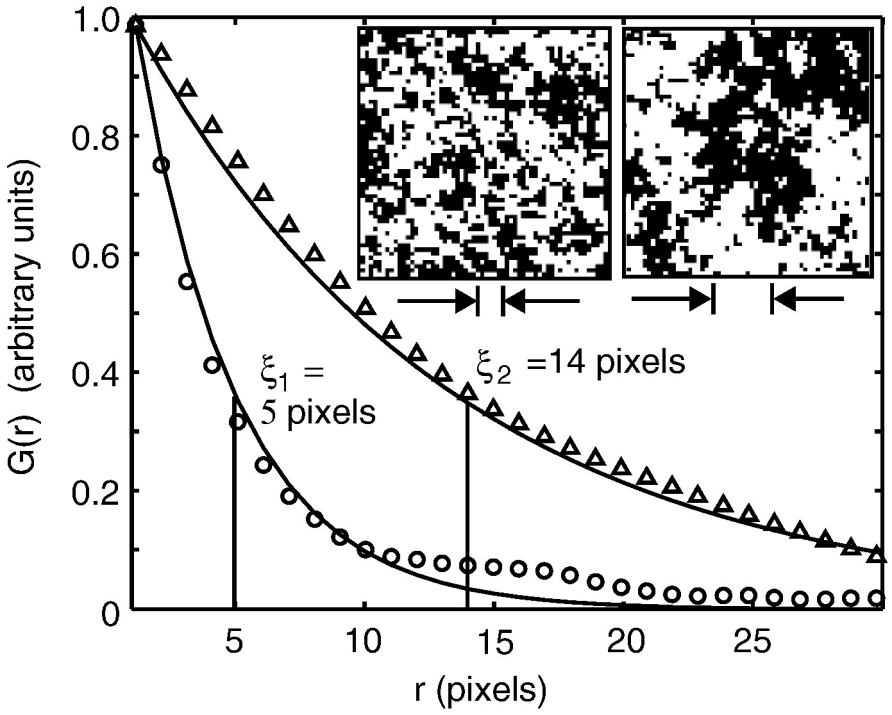

Figure 3.

Insets show Ising model simulations conducted far above the critical temperature (left) and just above the critical temperature (right). The interaction parameter, J, has a value of $0.035k_BT$ and $0.0425k_BT$, respectively. The graph shows angular-averaged autocorrelation functions $G(r)$ vs. distance r, derived from the simulation images, where data from the left inset are plotted as circles, and data from the right as triangles. Correlation length, ξ, is defined by fitting to $G(r) \propto e^{-r/\xi}$, as shown by the solid line. The fit is conducted over the entire range of r in the simulation, but only shown for $r < 30$. The correlation length for each simulation is indicated by the distance between the arrows below each image. The high-temperature simulation has a correlation length of about 4 pixels (or lattice spacings). In contrast, the autocorrelation function for the system near a critical point decays more slowly, with a larger correlation length of ~14 pixels, reflecting the presence of long-distance correlations between points.

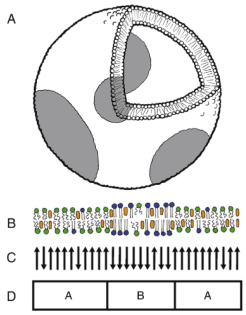

Figure 4.

(A) A unilamellar vesicle is a thin spherical shell composed of a lipid bilayer, bounded by water on the inside and outside. When the composition of the bilayer is a ternary mixture of a lipid with a high melting temperature, a lipid with a low melting temperature, and cholesterol, the bilayer can contain micron scale coexisting liquid phases. (B) The two liquid phases contain different mole fractions of the three lipid types. For a “giant unilamellar vesicle” of radius >20 microns, the lipid bilayer is essentially locally flat. The critical behavior of this membrane is well described by (C) a 2-D lattice of “Ising spins” or (D) any equivalent thin sheet of material containing two states as long as the correlation length is greater than the thickness of the sheet. It is not helpful to picture the spins as electrons paired in an atomic orbital, or as electrical dipoles, which behave differently than the Ising spins described here.

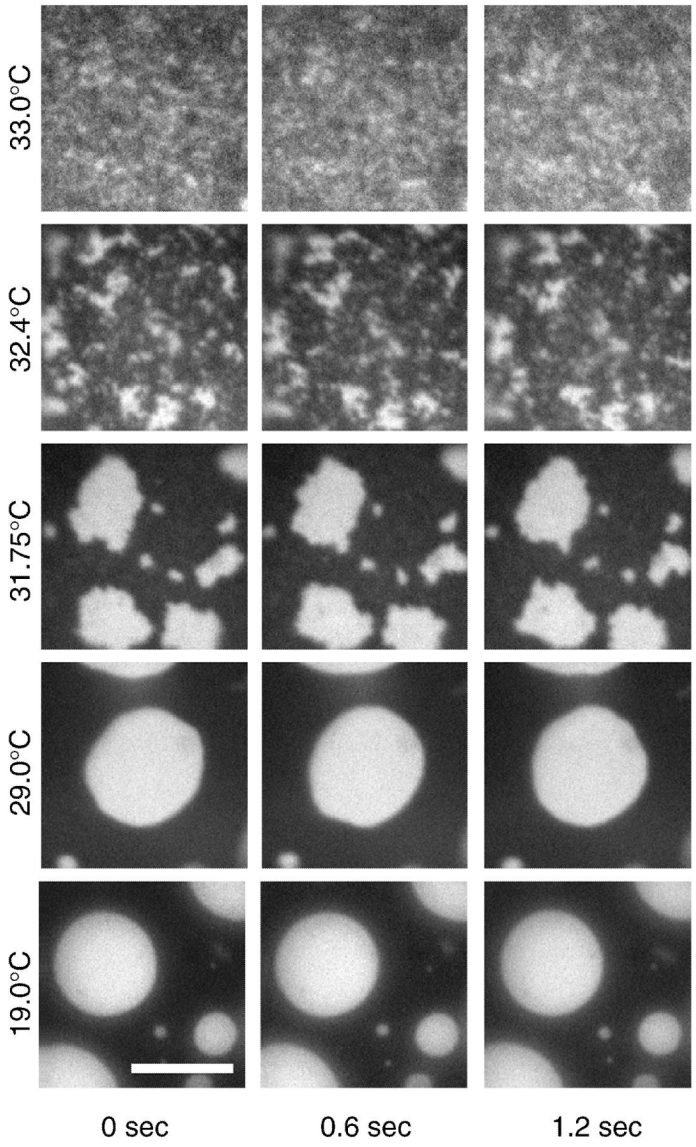

Figure 5.

Section of a membrane of a single giant unilamellar vesicle through time, at a series of temperatures. The membrane has a critical temperature of T_c~31.9°C. At 33.0°C, short-lived composition fluctuations are present. At 32.4°C, the fluctuations are larger and persist longer but the membrane remains homogeneous on average through time. At 31.75°C, just below the critical temperature, the membrane contains domains with a wide distribution of sizes. At 29.0°C, thermal fluctuations cause capillary waves which appear as rough domain edges. At 19.0°C, line tension is higher and domain edges are smooth. The vesicle was made and imaged as described previously (12). The vesicle is composed of 25:20:55 mol% of diphytanoyl phosphatidylcholine, dipalmitoyl phosphatidylcholine and cholesterol, with 0.8 mol% of the dye Texas Red dipalmitoyl phosphatidylethanolamine. Scale bar is 20 μm. The area shown in each image represents only ~4% of the vesicle surface area.

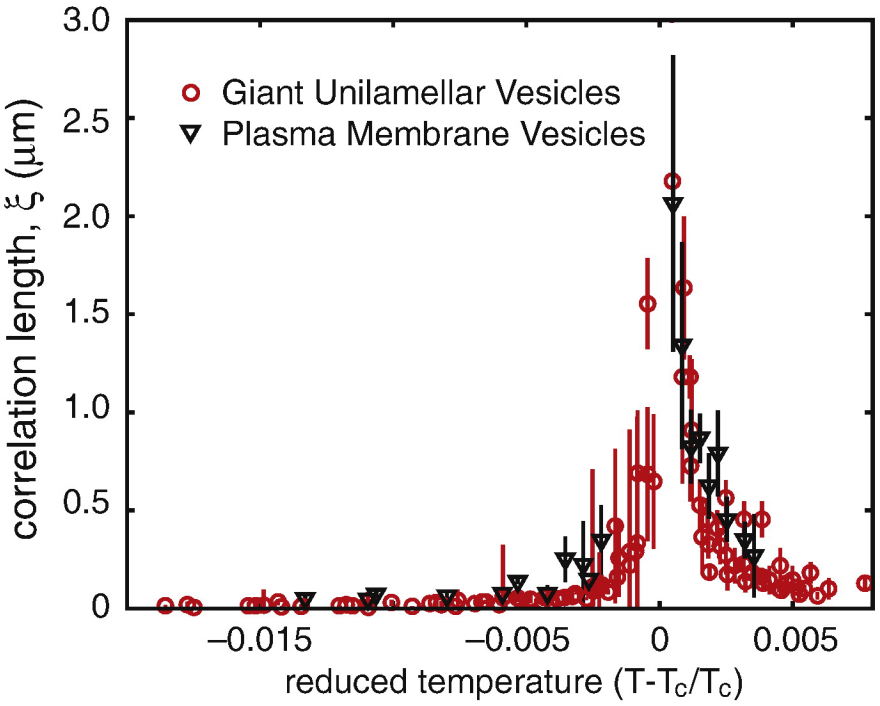

Figure 6.

Diverging correlation length, ξ, vs. reduced temperature $T_r = (T-T_c)/T_c$ for five different giant unilamellar vesicles (gray circles) and a single plasma membrane vesicle (black triangles). Equivalent data were published previously in figure 5 of (12) and figure 3 of (11). The data sets superimpose well, even though the compositions of the two membrane systems are different. For temperatures below T_c, we have used $\xi = (k_B T_c)/\lambda$, as described in (12).

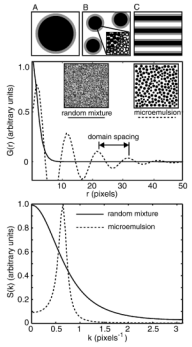

Figure 7.

Top: Sketches of an emulsion (A), microemulsion (B), and lamellar phase (C) in which grey surfactant molecules line the boundary between the white and black phases. Middle: Autocorrelation functions $G(r)$ for a disordered fluid (solid line) and a microemulsion (dashed line) are plotted vs. distance r from the functional forms given in reference (42). The insets are illustrative sketches. Bottom: Structure factors $S(k)$ are obtained by transforming the autocorrelation functions shown in the middle panel.

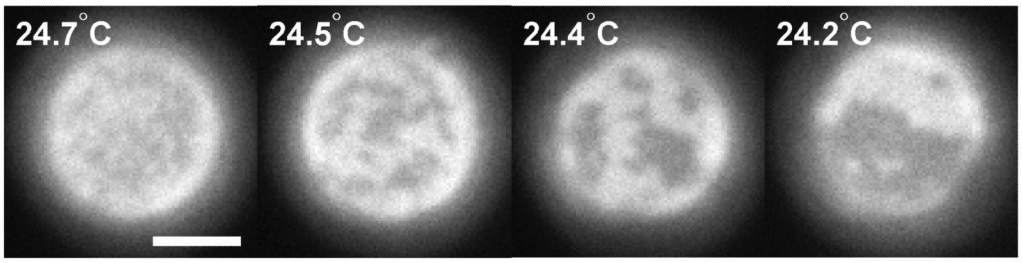

Figure 8.
Critical fluctuations are observed in giant plasma membrane vesicle (GPMV) prepared as described in reference (11) and fluorescently labeled with the fluorescent dye diIC12. The vesicle's critical temperature is ~24.3°C. The scale bar is 5 microns.

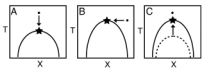

Figure 9.

Three mechanisms for approaching a critical point as shown in figure 1d. (A) Temperature is changed at a constant membrane composition. (B) The ratio of existing lipids in a membrane is changed at constant temperature. (C) Introduction of new membrane components or crosslinking of lipids or proteins shifts the phase boundary to a higher temperature.

TABLE 1

Static exponents characterize variables that do not change through time, such as susceptibility, specific heat, and the distribution of correlations. Exponents are taken from (25; 26). Additional exponents and further explanation can be found in the chart in reference (18). Each exponent applies to all systems within the same universality class (e.g. 2-D Ising). An exponent of 0 denotes logarithmic dependence. Dynamic exponents, which are not shown here, characterize the time dependence of variables, and each exponent depends on the details of each system (e.g. 2-D Ising with or without conserved order parameter) (106).

Measured quantity	Static Exponent	2-D Ising prediction	3-D Ising prediction	Mean field prediction
Specific heat	α	0	0.110(5)	0
Order parameter	β	1/8	0.325±0.0015	1/2
Susceptibility/Compressibility	γ	7/4	1.2405±0.0015	1
Shape of critical isotherm	δ	15	4.82(4)	3
Correlation length	ν	1	0.630(2)	1/2
Asymptote of correlation function	η	1/4	0.32±0.003	0
Line or surface tension	$\mu = (d - 1)\,\nu$	1		